

RESEARCH

Open Access



Optimization and preparation of in-situ mucoadhesive gel of azithromycin hydroxypropyl- β -cyclodextrin inclusion complex against upper respiratory tract infections

Jitu Halder¹, Shuvam Mishra¹, Ivy Saha¹, Ajit Mishra¹, Ritu Mahanty¹, Vineet Kumar Rai¹, Deepak Pradhan¹, Rakesh Kumar Sahoo¹, Salim Manoharadas², Muralidhar Tata³, Biswakanth Kar¹, Goutam Ghosh¹ and Goutam Rath^{1,4*}

Abstract

Background Azithromycin (ATM) has limitations, such as poor oral bioavailability and gastrointestinal (GI) side effects that restrict its widespread application.

Objective To develop a localized hydroxy propyl β -cyclodextrin (HP- β CD) inclusion complex-based in situ pH-responsive mucoadhesive gel of azithromycin (ATM) and evaluate its performance for the treatment of upper respiratory tract infections (URTIs).

Methods According to the phase solubility diagram, the ATM HP- β CD complex was prepared and analyzed by FT-IR, DSC, and SEM. Then, using a quality-by-design approach, pH-responsive in-situ gel was prepared. It was characterized in terms of their gelling capacity, pH, spreadability, swelling index, rheological properties and antimicrobial potential.

Results ATM HP- β CD complex 20-fold increased solubility of ATM, i.e., $49.84 \pm 1.39 \mu\text{g/mL}$ with improved dissolution profile compared to pure ATM. Optimized formulation characterized by its gelation pH (6.7), time (1.59 min), and viscosity (1607.9 Pa.s). The developed gel showed a good spreadability index ($322.6 \pm 0.5\%$), swelling index ($98.26 \pm 1.54\%$ after 10 h) and mucoadhesive strength (589 g/cm^2). Also, it exhibits a sustained drug release profile for 12 h ($94 \pm 1.37\%$) and a broader zone of *Staphylococcus aureus* growth inhibition ($31 \pm 3.54 \text{ mm}$).

Conclusion The developed mucoadhesive in situ gels demonstrated promising in vivo performance, primarily due to their effective antimicrobial activity. In vivo, local retention studies confirmed that the formulations adhered to the throat mucosa and remained in place for up to 24 h after application. The findings presented here suggested that this localized delivery system could serve as a useful strategy for improving the therapeutic effects of ATM against URTIs.

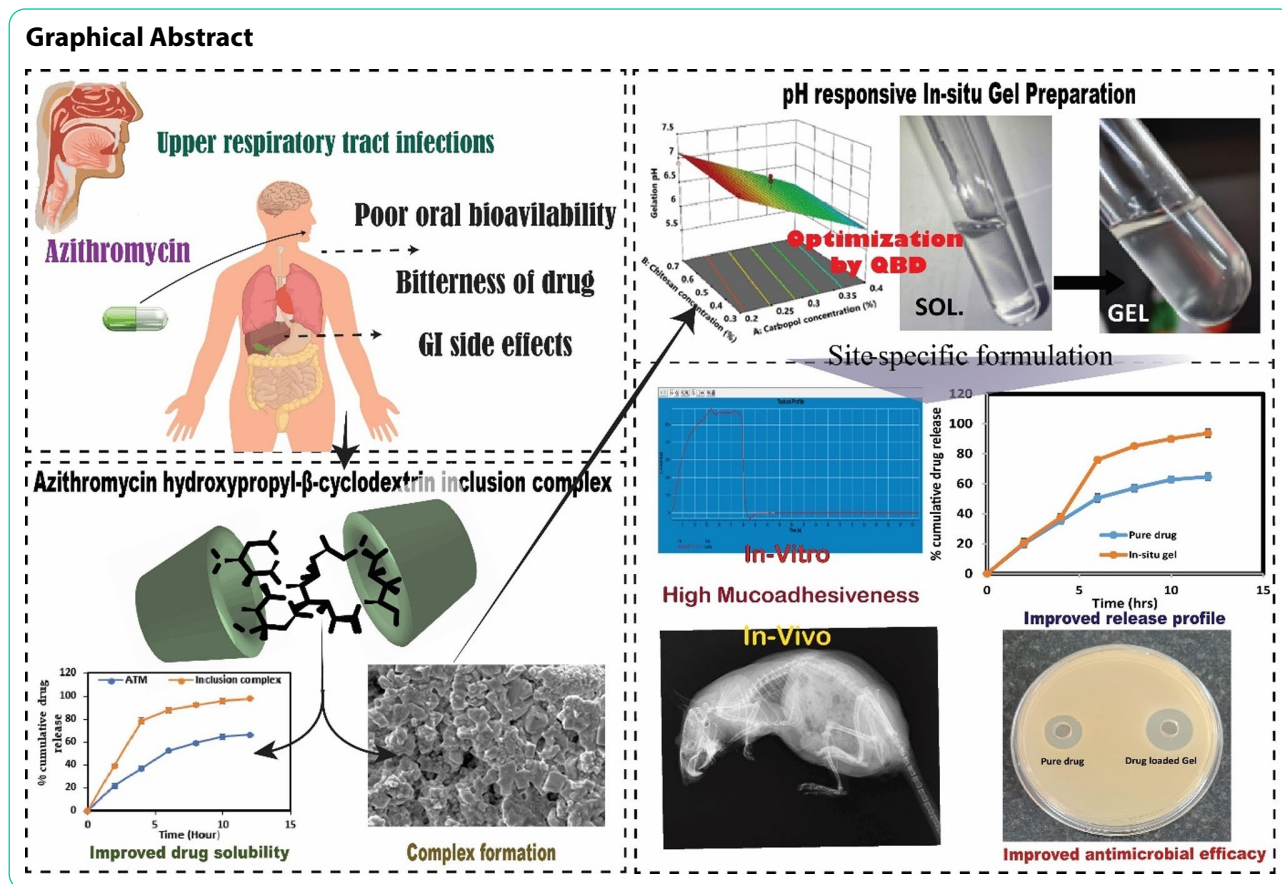
Keywords Hydroxypropyl β -Cyclodextrin, Inclusion complex, pH-responsive gel, Mucoadhesive gel, Upper respiratory tract infections

*Correspondence:
Goutam Rath
goutamrath123@gmail.com

Full list of author information is available at the end of the article



© The Author(s) 2025. **Open Access** This article is licensed under a Creative Commons Attribution-NonCommercial-NoDerivatives 4.0 International License, which permits any non-commercial use, sharing, distribution and reproduction in any medium or format, as long as you give appropriate credit to the original author(s) and the source, provide a link to the Creative Commons licence, and indicate if you modified the licensed material. You do not have permission under this licence to share adapted material derived from this article or parts of it. The images or other third party material in this article are included in the article's Creative Commons licence, unless indicated otherwise in a credit line to the material. If material is not included in the article's Creative Commons licence and your intended use is not permitted by statutory regulation or exceeds the permitted use, you will need to obtain permission directly from the copyright holder. To view a copy of this licence, visit <http://creativecommons.org/licenses/by-nc-nd/4.0/>.



Introduction

Sore throat and URTIs are prevalent complaints across all age groups [1]. Acute respiratory tract infections and URTIs account for roughly about 20–40% of outpatients and 12–35% of inpatients [2]. Among all respiratory infection episodes, nasopharyngitis, pharyngitis, tonsillitis, and otitis media comprised 87.5% of cases [3]. The primary cause behind strep throat or a sore throat is group A β -hemolytic *Streptococcal pharyngitis* [4]. Similarly, URTIs are caused by an array of microbes, including *Haemophilus influenzae*, *Staphylococcus pneumoniae*, *Staphylococcus aureus*, *Chlamydia pneumoniae*, *Mycoplasma pneumoniae*, and *Mycobacterium avium* complex [5]. Acute rheumatic fever and post-streptococcal glomerulonephritis are post-infectious consequences of ineffective *S. pyogenes* infection treatment [6]. Traditionally, oral penicillin was employed to treat these infections, but nowadays, macrolides are used preferentially due to high allergic reactions of the oral penicillin [7]. Amongst macrolides antibiotics, azithromycin is the most widely used macrolide; derived from erythromycin is effective against both gram-positive (*Staphylococcus pyogenes*) and gram-negative (*Haemophilus influenzae*) bacteria [8]. Despite its advantage, ATM has certain limitations, notably a lipophilic nature, which renders its

oral bioavailability poor (37%), and concomitant administration of ATM with food that drastically reduces drug absorption by 50% [9]. Additionally, it has a huge distribution volume of around 25 to 35 l/kg and a terminal half-life of about 68 h [9]. These suggest that ATM is being accumulated in healthy tissues, which can result in a lack of drug depot at the target site [10]. The majority of ATM adverse events are gastrointestinal in nature, resulting in stomach upset, loose stools (diarrhoea), vomiting, abdominal pain, indigestion, and gas [11]. It is already known that ATM is a macrolide antibiotic whose mode of action is to bind to the 23 S rRNA of the bacterial 50 S ribosomal subunit [12]. So, a unique, more site-specific formulation may demonstrate its efficacy in low-dose preparations and might minimize the side effects brought by conventional administrations.

As the traditional demand for high systemic dosages of drugs with low therapeutic indices elevates the risk of severe toxic side effects and the development of microorganisms that are resistant to the drug [13]. Thus, local administration of drugs might improve effectiveness while diminishing toxicity [14, 15]. Because of this, developing a novel site-specific formulation can combat ATM's challenges like high volume of distribution, low oral bioavailability, delayed onset of action, rapid distribution

from plasma to tissue, and an array of side effects [16]. Previously, pharmaceutical aerosols comprising of ATM were utilized in inhalation therapy to treat pulmonary infectious diseases [17]. However, this approach has several drawbacks, including the need for extremely tiny particles (1–5 μm), rapid drug clearance, drug disposal, and peripheral phagocytosis in the lungs [18]. As ATM in-situ mucoadhesive gel has been successfully used previously for ocular preparations which might be pH or thermosensitive [19, 20]. Thus, here, we are able to propose a unique novel site-specific formulation of ATM meant for its localized delivery in the mucosal region of the throat in the form of an in-situ mucoadhesive gel system as the pH of the eye and throat are approximately equal. Our afore-mentioned speculation has some obstacles, such as drug solubility [21]. There are various techniques or methods of solubility enhancement, including particle size reduction, salt formation, complexation, use of surfactants, solid dispersions, pH adjustment etc [22]. Here in the present research work, we opt for a method to improve the solubility of the drug by forming an inclusion complex with HP- β CD, which will additionally provide better stability [23].

In accordance with the statement, we aim to develop a Carbopol and chitosan-based pH-responsive in-situ gelling system for ATM delivery locally and characterize its efficacy against bacterial infection in-vitro, in-vivo. Localized delivery can manage dose-dependent systemic toxicity and also can elevate the drug's bioavailability, improving the therapeutic efficacy against bacterial infection.

Materials and methods

Materials

Azithromycin was received as a gift sample from Akums Lifesciences Limited, Sundran, Punjab 140,507. Chitosan was obtained from Merk Pvt. Ltd., Mumbai. Carbopol was procured from Lobachemie Pvt. Ltd, Tarapur, Palgarh, Mumbai. Hydroxypropyl- β -cyclodextrin were obtained from SRL Pvt. Ltd, Maharashtra. PBS solution and Agar broth were procured from Hi Media, Mumbai.

Preparation of standard curve of Azithromycin by UV-Vis spectroscopy

ATM (25 mg) was accurately weighed and transferred in a clean and dry 25 mL volumetric flask. The volume was made with phosphate buffer up to 25 mL, to produce a working solution of 1000 $\mu\text{g}/\text{mL}$. From this solution, 2, 3, 4, 5, and 6 mL were withdrawn separately in 10 mL volumetric flasks and volumes were made in each case made up to 10 mL with PBS (7.4) to produce concentrations of 200, 300, 400, 500, 600, $\mu\text{g}/\text{mL}$. The peak value of these solutions were recorded at λ -max 208 nm at UV-Vis spectroscopy [24].

Preparation of standard curve of Azithromycin by HPLC

A Shimazu LC System with a PDA detector performed the reversed-phase HPLC analysis. Methanol: water/ buffer (90:10, % v/v) was used in the mobile phase with a 1.5 mL/min flow rate at 210 nm wavelength [25]. The best stationary phase was determined as a C18 column, 5 μm , 250 mm \times 4.6 mm. The standard stock solution of ATM (10 mg/mL) was diluted accordingly to produce 100, 200, 400, 600, 800 and 1000 $\mu\text{g}/\text{mL}$ concentrations. The stock was diluted, and three replicate injections were performed into the HPLC. The general standard curve equation and the correlation coefficient (r) were obtained using the linear regression analysis.

Development of drug cyclodextrin inclusion complex

The solvent evaporation method was used to prepare the inclusion complex. Using a phase solubility investigation, the molar ratio of the drug and the complexing agent was optimized.

Phase solubility study

We adopted the Higuchi and Connors method to conduct the phase solubility investigation on a rotary shaker apparatus (Remi, India) at 350 rpm and $25 \pm 2^\circ\text{C}$ for 48 h in screw-capped vials with 25 mL of PBS (pH 7.4) solution of HP- β CD, ATM was added in a steady stream at ascending molar concentrations (0, 3, 6, 9, 12, and 15 mM). A preliminary inquiry led to establishing the stirring duration required to reach equilibrium. A Shimadzu UV/visible spectrophotometer measured the entire solution's drug content at 208 nm after achieving equilibrium before the solution was diluted accordingly and passed through a 0.25 μm membrane filter.

$$K_c = \text{slope}/S_0 \times (1 - \text{slope})$$

Where, S_0 is the solubility of ATM at pH 7.4, obtained using a UV/vis spectrophotometer at 208 nm, and the slope is the outcome of the linear regression [26].

Preparation of inclusion complex

Applying the solvent evaporation method, ATM and HP- β CD were incorporated in a 1:1 m ratio to formulate the inclusion complex (0.749 g of ATM and 1.540 g of hp-cd). Keeping the molar ratio 1:1, ATM and HP- β CD were dissolved in 50% (v/v) aqueous ethanol. The solution was agitated at 45°C until it became translucent, and then it was evaporated under vacuum. The solid wastes were ground into a dry complex and thoroughly dried for a further 48 h at 50°C before being sieved through sieve No. 80. The final samples were kept in a desiccator until they were desired [27, 28].

Characterization of the prepared inclusion complex

Solubility study

The saturation point in determining the solubility of ATM and its inclusion complex were evaluated in triplicate. Using a rotary shaker, an overweighed quantity of both samples was taken individually in two different flasks and blended into PBS (pH 7.4) for 24 h at room temperature (25 ± 2 °C). Both samples were then filtered, and a UV/Vis spectrophotometer was used to analyze them at 208 nm [29].

Fourier transform infrared spectroscopy

The IR spectra have been recorded via FTIR (Shimadzu, Japan). A disc that had been weighed and compressed contained 100 mg of KBr and 1 mg of sample. The disc was scanned from 4000 to 400 cm^{-1} in the spectral range, and spectral data was gathered [30].

Differential scanning calorimetry (DSC)

In the present investigation, DSC (Mettler Toledo) was employed for one of its traditional operations: determining whether the drug and the complexing agent potentially interact. 2–3 mg of sample were put into a 50- μl perforated aluminium pan, then tightly sealed. Heat runs were set for the sample to range from 4 to 400 °C, nitrogen served as a purging gas, and the sample was subsequently analyzed [31].

Morphology

The drug, and HP- β CD, and its inclusion complexes are analyzed to identify their shape. The morphology was confirmed using Scanning Electron Microscopy (SEM) (ZEISS, Evo 18, Thornwood, NY, United States). A small amount of powder coated with gold sputter was positioned in the SEM sample holder. SEM images were obtained with an acceleration voltage of 20 kV and the

magnification power was 20 kX. The objective was to investigate the distribution of exposed features and the dimensional topography [32].

In-vitro dissolution studies of inclusion complex

100 mg of pure drug (ATM) and an equivalent amount of inclusion complex were added to the dissolution media separately. The study was performed using the USP dissolution apparatus I (basket method) in 500 mL of 7.4 pH Phosphate buffer at 37 ± 1 °C and 50 rpm for 12 h. After each sampling, a 5 mL aliquot was taken out, and an equivalent quantity of fresh media was added into the flask to keep the sink condition. The sample was then scanned spectrophotometrically at 208 nm against a compatible blank using a UV-visible spectrophotometer. The % cumulative of ATM released from the inclusion complex was identified and demonstrated against time and compared with pure drug [33].

Statistical optimization of pH-responsive in-situ gel formulation

A two-level, two-factor central composite design was used to optimize the formulation. “Designing a statistical experiment was done with software DESIGN EXPERT® trial version 13.0 (Stat-Ease Inc., Minneapolis, USA)”. The factor interaction between the variables under consideration was presented using response surface graphs. Two specific independent variables that were examined were Carbopol 934 concentration (%w/w) (X1) and Chitosan concentration (%w/w) (X2). The values of two independent variables were coded as low, medium and high levels (-1, 0 and +1, respectively). The screened, most critical dependent variables being investigated were- gelation pH (Y1), gelation time (Y2) and viscosity (Y3). A total of 13 (Table 1) experimental batches were suggested by the software to analyze the effect of each level on formulation characteristics and to optimize the conditions required to fabricate the formulation with maximum efficiency. Results obtained from batches with different levels of independent variables were put into software for analysis and further optimization [34, 35].

Optimization

Based on terms from the ANOVA, the software produced a statistical polynomial equation. There were 13 runs produced, 5 of which had center points. A statistically significant coefficient and a r^2 value were used to evaluate the model. Validated RSM results were discovered to be accompanied by the compositions of optimized formulation throughout the complete trial region. It was programmed with a gelation pH of 5.7 to 7, gelation time of 0.9 min to 3 min, and viscosity between 1007 and 2200 Pa will be the best batch. Different levels and variables used in central composite design are given in Table 2.

Table 1 Experimental runs suggested by design expert software

Run	X1 Carbopol concentration %	X2 Chitosan concentration %
1	0.4	0.7
2	0.3	0.5
3	0.3	0.5
4	0.3	0.5
5	0.2	0.7
6	0.4	0.3
7	0.3	0.5
8	0.2	0.3
9	0.3	0.782843
10	0.3	0.5
11	0.3	0.217157
12	0.158579	0.5
13	0.441421	0.5

Table 2 The experimental conditions for the optimization of pH-responsive in-situ gel

Variables	Level of variables				
Independent	-α	-1	0	+1	+α
X1 = Concentration of Carbopol 934 (%w/w)	0.15	0.2	0.3	0.4	0.44
X2 = Concentration of Chitosan (%w/w)	0.21	0.3	0.5	0.7	0.78
Response	Dependent				
Y1 = Gelation pH	5.7- 7				
Y2 = Gelation time	0.9–3 min				
Y3 = viscosity	1007–2200 Pa.s				

Data analysis and validation of response surface methodology

These findings were made in a way that they can be used by the “Stat-Ease’s Design-Expert software to analyze various independent variables’ impact on response factors by employing multiple linear regression analysis (MLRA)”. A polynomial model was then developed through the software. These models were confirmed using Analysis of Variance (ANOVA). “In turn, these equations generated by the software needed to be re-visited and checked against the critical material attributes they affected. The software also generated 3D response surface plots, 2D perturbation curves and contour plots to visualize the main interaction effects of the variable”. Based on this approach, goals were set, and checkpoint batches were made using the desirability option of the software to identify CMA composition to achieve a critical quality attribute target. Then, the highest desirability level prediction was selected and compared with experimental results against predicted values [34].

Formulation of in-situ mucoadhesive gel

Optimize chitosan concentration was dissolved in 20mL of acetate buffer (pH 4.6) to develop the in-situ gelling system. The appropriate concentration of Carbopol 934 was dispersed in double distilled water while stirring continuously using a mechanical stirrer (Remi instruments, India) until a uniform mixture was achieved. After that, both the polymeric solutions are mixed together. Under aseptic circumstances, an equivalent to 0.5% azithromycin containing inclusion complex powder was added to the aforementioned polymeric solution. In order to optimize the compositions as in situ gelling systems, prepared formulations were examined for their gelation pH, gelation time and viscosity. The gelling capability was assessed by adding 0.5 mL of the freshly produced PBS to a vial containing 2 mL of the polymeric system, which was equilibrated at 37 ± 1 °C. The viscosity was determined by utilising a Brookfield viscometer and a tiny volume adapter [36].

Characterization of the optimised in-situ mucoadhesive gel system

General appearance

The optimized formulation was subjected to visual examination to ascertain the physical appearance of mucoadhesive gel as well as its texture (organoleptic properties including colour, transmittance, and phase separation) [37].

Determination of pH

A petri dish holding 3 g of the gel was filled in order to gauge its surface pH. More than 5 mm of the pH meter’s (Elico) electrode was submerged in the mixture for a period of 5 min [38].

Rheological studies

The optimized formulation with a pH of 5.9 was added to the Brookfield Synchroelectric Viscometer’s small sample adaptor, and the angular velocity increased progressively from 10 to 100 rpm or 0.16 to 1.66 S^{-1} . Dial reading was noted. After pouring phosphate buffer into the mixture to get the gelation at pH level 7.4, it was poured into an ointment jar. The dial reading was once more noted and utilized to determine the viscosity of the in-situ mucoadhesive gel system [38].

Spreadability

The spreadability of a formulation is its ability to spread after gel formation, which can be measured utilizing an in vitro setup. For this, a circle of 4 cm (starting diameter) on an uncontaminated, dried glass surface was marked with a quantity of 2 g of the gel. A mass of 500 g was placed on two glass surfaces, one on the top of the gel, for 5 min. Using the following equation, the expansion in diameter (final diameter) was calculated [39].

$$\text{Spreadability (\%)} = \frac{\text{Final diameter}}{\text{Initial diameter}} \times 100$$

Swelling index (SI) and matrix erosion (ME)

In order to measure SI, 2 g of the optimized formulation (W1) was kept on a glass slide that had already been submerged in a Petri plate filled with 10 mL of PBS (pH 7.4). The entire system was put into an incubator oven at 37 ± 1 °C for the entire course of the experiment. Through the application of an electronic weighing balance, the increase in weight of the formulation over time was measured in intervals and denoted by W2, and the SI at every time interval was estimated utilizing the following equation [40].

$$SI = \left(W2 - \frac{W1}{W1} \right) \times 100$$

Like that, for computing ME, the swollen formulation was maintained at 60 °C for 24 h until a steady weight (W3) was reached. Then ME was then calculated using the following equation.

$$ME = \left(W1 - \frac{W3}{W1} \right) \times 100$$

Ex-vivo mucoadhesiveness

The detaching force necessary to pull apart the in-situ gel from goat throat mucosa was estimated utilizing a texture analyzer (Brookfield texture analyzer (V1.3 Build 15; Brookfield Engineering Labs, Inc). A newly dissected portion of goat throat mucosa, measuring 2 cm by 2 cm, was initially allowed to acclimatize to 37.0 °C in a buffer with a pH of 7.4. Part of the mucosa was affixed to the apparatus's top assembly with its mucosal surface facing outward, while the lower assembly received a pre-determined dosage of gel (500 mg). The top probe was gradually moved downwards into the bottom assembly, keeping a constant rate of movement till it came in contact with the lower assembly, applying a force of 1 N for 60 s. After that, the probe was moved apart and upwards for a distance of 15 mm with a speed of 0.5 mm/s. The force needed to pull apart the gel from the mucosa was recorded [34, 41].

In-vitro drug release

Employing the dialysis tube method, the in vitro release profile of ATM from the optimised in situ gel was investigated. A dialysis bag with 5 g of the optimized formulation was placed in a beaker containing 500 mL of PBS pH 7.4 (Receptor medium). The beaker was positioned over a magnetic stirrer, which was kept running at 50 rpm and 37 ± 1 °C. At a particular time interval, 5 mL of aliquot was taken out and replaced with a comparable amount of fresh receptor media. The aliquots have been analyzed at 208 nm using a UV spectrophotometer [42, 43].

In-vitro anti-microbial activity

The organism that causes throat infections, *Staphylococcus aureus*, was used in tests to determine the formulations' therapeutic potential, or more specifically, the optimised formulation's antimicrobial activity. The potato dextrose agar medium was equally spread across a 100 µl aliquot of the bacterial suspension. Agar gel that had previously been set using an in situ ATM HP-β-cyclodextrin complex corresponding to 175 mg of pure medication and a straightforward ATM solution. The plates were incubated at 37 ± 1 °C for 48 h [44].

MIC determination

The standard broth dilution method was employed to assess the antimicrobial effectiveness of the in situ gel containing the ATM HP-β-cyclodextrin complex by observing microorganism growth in agar broth. To determine the minimum inhibitory concentration (MIC) in broth, serial dilutions of the formulations free drug were prepared, with ATM concentrations ranging from 5 µg/mL to 0.1 µg/mL, alongside a bacterial concentration adjusted to 10 × 10⁸ CFU/mL (0.4 McFarland's standard). A control, consisting of only inoculated broth, was incubated for 24 h at 37 °C. The MIC endpoint was identified as the lowest concentration of the formulation, and no visible growth was observed in the tubes. The turbidity of the tubes was observed both before and after incubation to verify the MIC value.

In-vivo characterization of the optimised in-situ mucoadhesive gel system

Ethics statement

We have our own approved Institutional Animal Ethics Committee (IAEC) registration number **1171/PO/Re/S/08/CPCSEA** (New Delhi, India). The animals were procured, and the experiments were conducted at the Laboratory Animal Facility of the School of Pharmaceutical Sciences, Siksha "O" Anusandhan (Deemed to be University). Twenty male albino rats, weighing 210–250 g, were housed in the animal room for the study. The research complied with the latest CPCSEA India Guidelines and the EU Directive 2010/63/EU for animal studies. The study protocol, designated as "**IAEC/SPS/ SOA/122/2022**," received prior approval from CPCSEA via the Institutional Animal Ethics Committee before initiating the research.

In-vivo antimicrobial challenge study

The *Staphylococcus aureus* model was utilized to induce the disease. To prepare the inoculum, the organisms were cultured on potato dextrose agar and transferred to the appropriate medium. The bacterial count was standardized using the McFarland scale (0.5 McFarland standard), equating to approximately 10⁶ CFU/mL. A suspension of the test microbes in sterile 0.9% normal saline was prepared and diluted to match this standard. For the experiment, 0.1 mL of the suspension (approximately 2 × 10⁵ CFU) was inoculated orally into anaesthetized rats. Anesthesia was achieved by giving intramuscular injections of ketamine and xylazine in a ratio of (90:10) mg/kg of body weight. During anaesthesia, the rats' body temperature was maintained at 38 °C using a regulated heating pad until they recovered. Daily survival monitoring was conducted, and samples were collected on days 3, 5, and 7. The number of viable bacteria in the respiratory was determined by plating serial dilutions of the samples

on potato dextrose agar plates, followed by incubation at 37 °C for 24 h. Colonies were counted to calculate CFU/mL. After disease induction, infected rats received treatment with developed ATM in-situ gel (Gel equivalent dose of 5 mg/kg of ATM), and marketed formulations of ATM at a dose of 5 mg/kg. The solution is directly placed into the animal's mouth using a feeding needle. Samples were collected 24 h post-dosing via mucosal swab to determine the viable bacterial count.

In vivo retention and analytical Estimation study

The retention efficacy of the optimized formulation in rats was evaluated using radiographic imaging. Prior to the experiment, the animals were fasted overnight but allowed free access to water. The formulation, containing 0.50% barium sulfate as a contrast medium, was orally administered using pan-century insufflators. X-ray images of the throat were captured at various intervals over 24 h to monitor the spray-dried nanoparticles' in vivo movement and behavior. The X-ray imaging was conducted with an L&T Vision 100 (C-arm) X-ray machine, operating at 64 mAs and 63 kV [45].

Further, mucoadhesive drug retention at the oral mucosa was analyzed for bio-analytical estimation by HPLC [46]. The study involved a group of six animals that received a mucoadhesive in situ gel formulation of ATM (5 mg/kg). Throughout the experiment, the animals were provided with sterile water and food daily, following a 15-day washout period prior to the study. Swab samples (0.5 mL) were collected at specific time intervals: 1, 4, 8, 12, 18, and 24 h post-administration. These serum samples were analyzed for bio-analytical estimation.

Statistical analysis

The data were statistically analysed using Graph-Pad Prism instate. A one-way analysis of variance was employed to compare variance amongst the groups. $P=0.05$ was used to determine statistical significance ($n=3$).

Result and discussion

Standard curve of ATM

The standard curve (Fig. 1a) of ATM was plotted in pH 7.4 phosphate buffer, and absorbance was taken at 208 nm. The standard plot of ATM in pH 7.4 phosphate buffer showed considerably good linearity with an R^2 value of 0.9989 in the concentration range of 200–600 µg/mL. The calibration curve of ATM was prepared at λ_{\max} 210 nm using HPLC, and regression (r^2) was found to be (0.995). Linearity was found to be in the 100 to 1000 µg/mL concentration range. Figure 1b represents the standard curve obtained using HPLC; ATM's retention time was found at 2.40 min.

Development of the inclusion complex

Phase solubility study

According to the phase solubility graph, ATM's aqueous solubility followed the first order regarding the HP-βCD (ligand) concentration, as indicated in Fig. 1c. It was discovered that the plot was AL-type. So, this phenomenon indicated a 1:1 molar ratio for ATM complexation with HP-βCD. The apparent stability constant of ATM was found to be $5.98 \times 10^4 \text{ M}^{-1}$, indicating that the inclusion complex was stable.

Preparation of inclusion complex

ATM inclusion complex was formulated using the solvent evaporation method with a 1:1 molar ratio of a complexing agent such as HP-βCD. The percentage drug content value was determined through an assay to be $98.22 \pm 0.25\%$ ($n=3$).

Characterization of inclusion complex

Solubility study

Pure ATM possesses a saturated solubility of $2.4 \pm 1.04 \text{ µg/mL}$ in distilled water, but the inclusion complex has a solubility of $49.84 \pm 1.39 \text{ µg/mL}$, a boost of approximately 21-fold. This outcome suggests that ATM molecules have entered the HP-βCD cavity. Similar results have been achieved by Shah et al. in an attempt to enhance the solubility of itraconazole [47].

FT-IR spectroscopy

A comparison was made between the complex's FT-IR spectrum and that of pure drug and HP-βCD (Fig. 2a). The spectrum exhibiting the inclusion complex revealed distinct peaks for both HP-βCD and pure drug, signifying the formation of the inclusion complex in the absence of any chemical alteration. "The FTIR spectra of pure ATM showed characteristic peaks at 1368.72 cm⁻¹ (C-N-stretching), 2958.90 cm⁻¹ (C-H-stretching), 1379.15 cm⁻¹ (C-HO-stretching alcoholic group), 1545.03 cm⁻¹ (C=O-stretching amidic group), 3471.98 cm⁻¹ (N-H-stretching), 1707.06 cm⁻¹ (C=C-bending), 794.70 cm⁻¹ (C-F-stretching), 1122.61 cm⁻¹ (OH- bending)". The inclusion complex and ATM had identical fundamental peaks and patterns in FTIR spectra. Thus, no significant interaction exists between the drug and excipients. The presence of -1122.61 cm⁻¹ (OH- bending), and 1545.03 cm⁻¹ (C=O-stretching amidic group), respectively, in ATM and HP-βCD complex indicates the chemical stability of ATM in HP-βCD complex.

DSC thermogram

The DSC thermograms of pure HP-βCDs, ATM, and inclusion complex are shown in Fig. 2b. In this study, DSC was applied for one of its more traditional purposes, which involved looking at potential interactions between

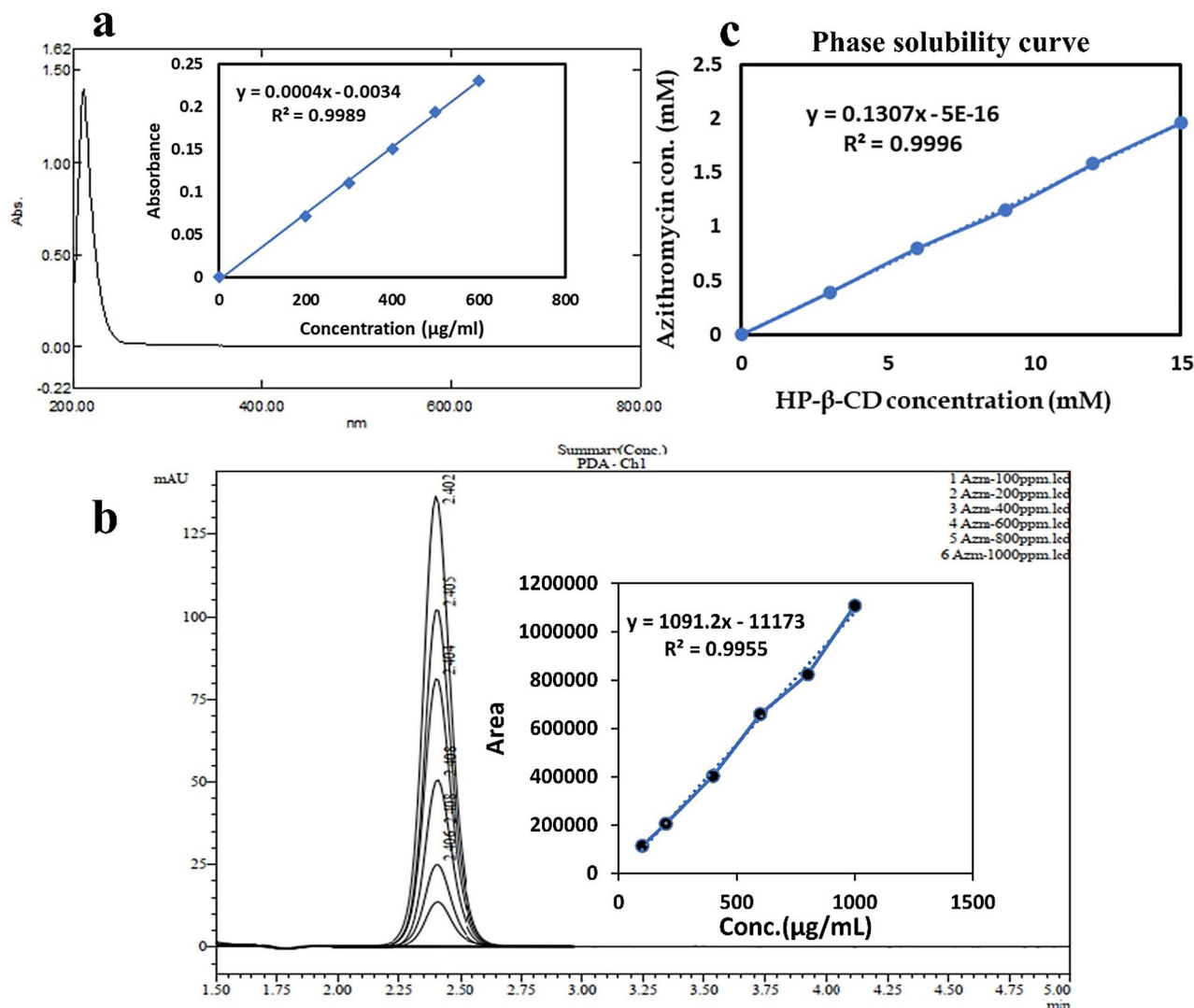


Fig. 1 (a & b) Calibration curve of azithromycin in pH 7.4 phosphate buffer at 208 nm and Calibration curve of azithromycin by HPLC at 210 nm. (c) Phase solubility curve of azithromycin

a drug and the excipients being employed. DSC thermograms for pure drug, HP- β CDs, and inclusion complex displayed endothermic peaks at the corresponding melting points. A sharp characteristic endothermic peak appeared on the ATM thermogram at 126.43 $^{\circ}\text{C}$, indicating the substance's purity. Compared with pure ATM and HP- β CD, the DSC curves of inclusion complexes displayed completely different peak patterns: the endothermic fusion peak disappeared at 126.43 $^{\circ}\text{C}$ and new peaks appeared at 106.21 $^{\circ}\text{C}$ and 134.82 $^{\circ}\text{C}$. This small shifting may be due to the phase transition during the complex formation. The results indicated strong interactions between ATM and the HP- β CD in their inclusion complexes.

Morphology

Figure 3a shows the morphology and surface properties of the ATM and inclusion complex that were studied using a scanning electron microscope. The prepared ATM HP- β CD inclusion combination manifested as amorphous particles. This is because the inclusion complex allows limited drug molecules into it, which cannot form a stable crystal and improve the solubility of drug molecules. The morphological study revealed that ATM crystals were rod-shaped, while the inclusion complex had an irregular, block-like structure, confirming the successful formation of a different solid phase. This indicating that the complex was successfully formed [48].

In vitro dissolution study of the inclusion complex

The pure drug and the inclusion complex (1:1 m) produced via the solvent evaporation method underwent the

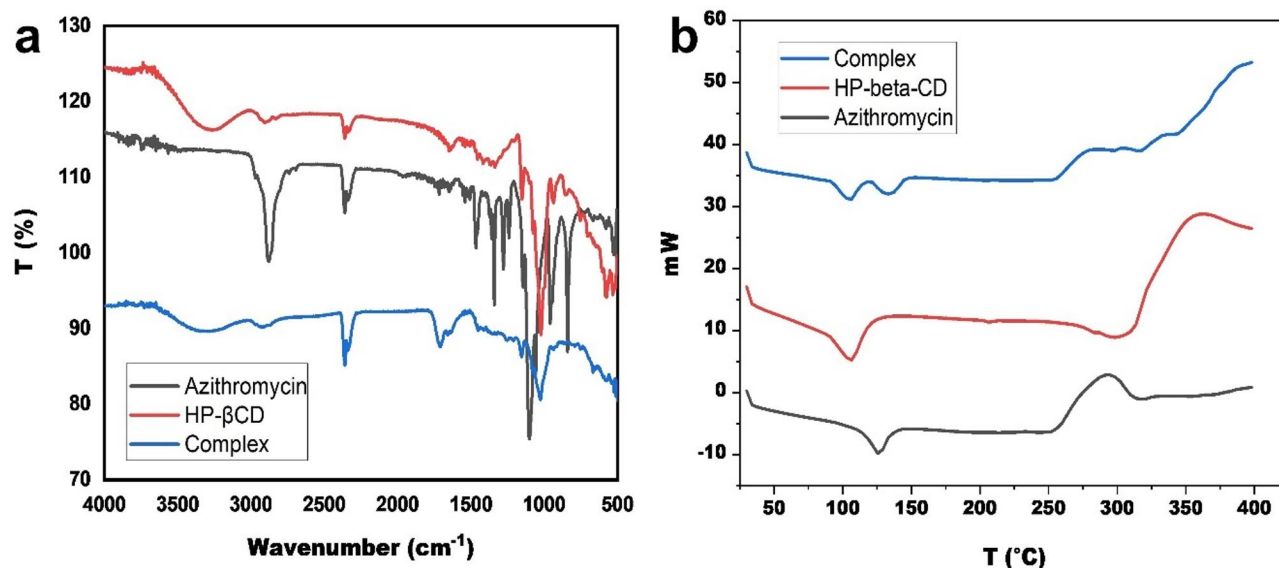


Fig. 2 (a) FTIR Spectra and (b) DSC thermogram of pure drug, HP-βCD and inclusion complex

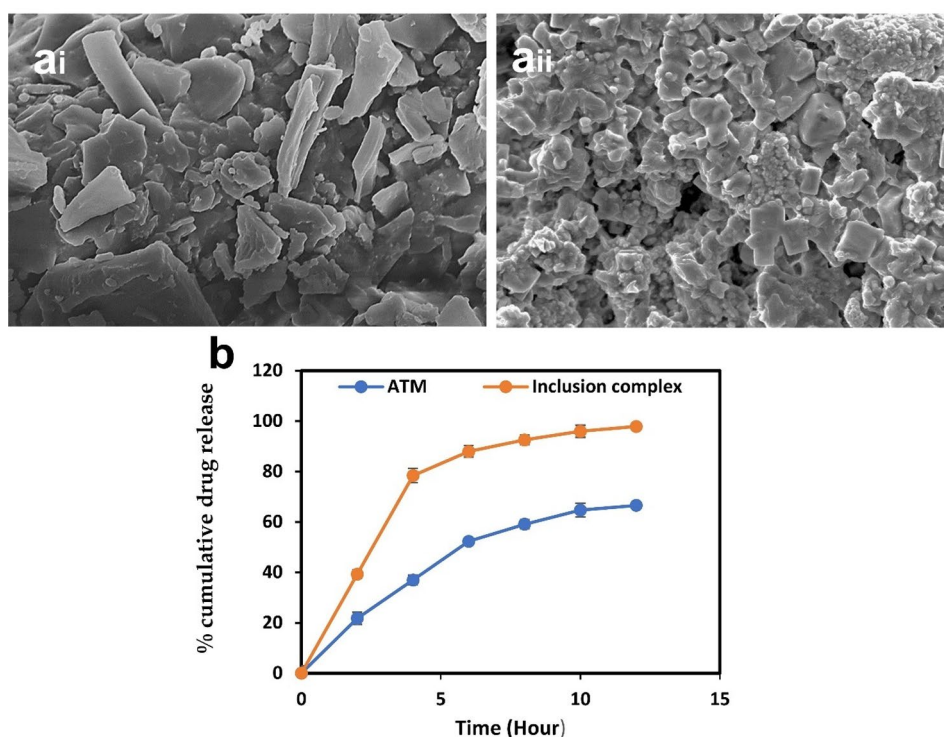


Fig. 3 Scanning electron microscopical images of Azithromycin (a.i.) and Azithromycin HP-βCD complex (a.ii). (b) Dissolution profile of Azithromycin (ATM) and Azithromycin HP-βCD inclusion complex

in-vitro drug release test. A graph (Fig. 3b) was plotted showing the cumulative percent drug released concerning time for two samples, with time in hours on the x-axis and % cumulative drug release on the y-axis. According to in vitro studies, the inclusion complex of ATM dissolves far more quickly than the pure drug (66.56%) does after 12 h. The inclusion complex showed an increase

in ATM dissolution, which could be attributed to the hydrophilicity of the cyclodextrin molecule that offers enhanced drug solubility [49]. The inclusion complex (made using the solvent evaporation method with a ratio of 1:1 molar ratio of drug and HP-β-CD) was determined to be approximately $98 \pm 2.06\%$, according to the in vitro drug release profile. This might be explained by the use of

complexing agents, which solubilize the drug and enable it to form a complex with the pure hydrophobic drug [50].

Optimization and development of pH-responsive in-situ gel

Carbopol 934 and chitosan are FDA-approved biocompatible tri-block polymers that are compatible with the drug and selected for the preparation of pH-responsive in-situ gel. Table 3 includes different combinations of factors chosen with determined values of dependent variables, i.e. gelation pH, gelation time, and viscosity.

ANOVA and interaction effect on gelation pH

This factor was fitted to the linear model, and the model's F-value turned out to be 24.92, which implies that the model is significant. Also, the P value was <0.0001, indicating that model terms are significant. The Lack of Fit F-value was observed to be 2.05, indicating that the Lack of Fit is not significant relative to the pure error. The predicted R² of 0.6949 was in good compliance with the Adjusted R² of 0.7995; i.e. the difference was less than 0.2.

Final equation in terms of coded factors

$$\text{Gelation pH (Y1)} = 6.51538 - 0.51731 * X1 + 0.0832107 * X2$$

It can be implied from the equation that the Carbopol concentration (X1) has a negative impact on the gelation temperature. This means the gelation pH was reduced with increasing Carbopol concentration. Whereas chitosan concentration (X2) positively affected gelation pH, X1 with a higher magnitude was discovered to have a maximum magnitude of negative impact. Carbopol

Table 3 Factor combination with determined value of dependent variables

Run	X1 Carbopol concentration %	X2 Chitosan concentration %	Y1 Gela- tion pH	Y2 Gelation time min	Y3 Vis- cos- ity Pa.s
1	0.4	0.7	5.9	2.2	1929
2	0.3	0.5	6.8	1.4	1400
3	0.3	0.5	6.4	1.2	1800
4	0.3	0.5	6.7	1.8	1700
5	0.2	0.7	6.9	3	1540
6	0.4	0.3	5.7	1.2	1756
7	0.3	0.5	6.5	1.6	1600
8	0.2	0.3	7	1.1	1321
9	0.3	0.782843	6.9	2	1730
10	0.3	0.5	6.7	2	1500
11	0.3	0.217157	6.5	0.9	1420
12	0.158579	0.5	7	1.65	1007
13	0.441421	0.5	5.7	1.5	2200

concentration and gelation pH had an inversely proportional relationship, which was also represented in the linear coefficient of X1's negative magnitude. The perturbation curve, contour, and 3D response surface plot (Fig. 4a, b and d) all indicate that the X1/A variable negatively impacted gelation pH variance up until the intermediate levels. Still, as their levels increased, the gelation pH significantly declined.

ANOVA and interaction effect on gelation time

This factor was fitted to the linear model, and the model's F-value was 11.11, which implies the model to be significant. Also, the P value was found to be 0.0029, indicating model terms are significant. It was discovered that the F-value for the lack of fit was 1.27, indicating that the lack of fit is not significant in relation to the true error. A significant Lack of Fit F-value has a 42.59% probability of being caused by noise. The Adjusted R² of 0.6276 and the expected R² of 0.4298 agreed reasonably well, with a difference of less than 0.2.

Final equation in terms of coded factors

$$\text{Gelation time (Y2)} = 1.65769 - 0.114017 * X1 + 0.556954 * X2$$

To explain the equation, Carbopol concentration (X1) negatively impacts the gelation temperature, while the chitosan concentration (X2) positively impacts gelation time. The higher magnitude of X2 implicated the positive impact on gelation time to be maximum. This means that the gelatin time increased when the Carbopol concentration was reduced, whereas gelation time was lessened when the chitosan concentration was reduced. As observed from the perturbation curve, contour and 3D response surface plot (Fig. 4d, e and f), X1/A negatively influences variance in gelation time, and X2/B has a positive impact up until the intermediate levels. According to the findings, lesser Carbopol percentages required much more time for gelation. A negative magnitude for the coefficient of X1 also indicated the inversely proportional relationship between Carbopol concentration and gelation time. To conclude, increased Carbopol percentages reciprocated earlier gelation.

ANOVA and interaction effect on viscosity

This factor was also fitted to the linear model, and the model's F-value was found to be 21.89, which implies that the model is significant. Furthermore, 0.0002 was found to be the P value, indicating the significance of the model terms. The F-value for the lack of fit was determined to be 0.66, meaning that the lack of fit is insignificant in relation to the true error. With a difference of less than 0.2, the adjusted R² of 0.7769 and the expected R² of 0.6861 were in reasonable agreement.

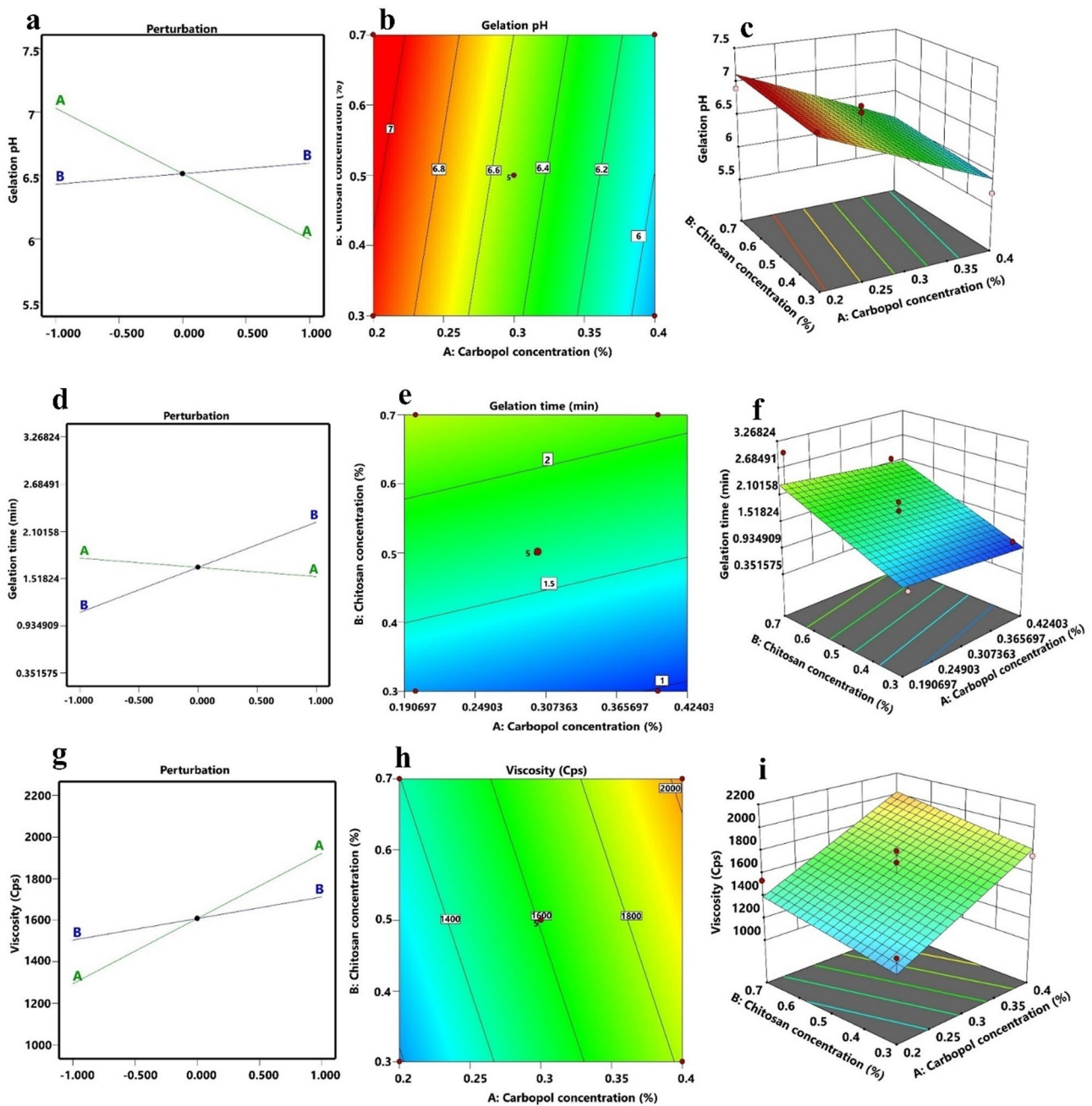


Fig. 4 Model graphs for Gelation pH, Gelation time, Viscosity (a, b, c) Perturbation curve, 2D contour plot and 3D Response surface plot for Gelation pH. (d, e, f) Perturbation curve, 2D contour plot and 3D Response surface plot for gelation time. (g, h, i) Perturbation curve, 2D contour plot and 3D Response surface plot for viscosity

Final equation in terms of coded factors

$$\text{Viscosity (Y3)} = 1,607.92 + 313.895 * X1 + 103.801 * X2$$

The formula shows that the viscosity is positively impacted by the chitosan (X2) and carbopol (X1) concentrations. The biggest favorable influence was found when the X1 magnitude peaked. This suggests that the

solution’s viscosity increases with increasing polymer concentration. The perturbation curve, contour plot, and 3D response surface plot (Fig. 4g, h, and i) indicate that both X1/A and X2/B have a favorable effect on gelation time variance up to intermediate levels. **Point prediction and validation of the model.**

The maximum desirability function and post-analysis point prediction capability of Design-Expert software were used to determine the ideal composition of the

formulation. The intended aim or goals for the required quality attributes were determined to be constraints, such as viscosity, gelation temperature, and gelation time. With the optimum amount of formulation components such as Carbopol concentration (X_1) = 0.3% and chitosan concentration (X_2) = 0.5%. At these levels of independent variables, the desired gelation temperature, time, and viscosity of in-situ gel can be obtained. The experimental observations from the checkpoint batch and the software-predicted values of dependent variables were compared. Observed and predicted gelation pH were determined to be 6.7 and 6.5, respectively, and predicted and experimental gelation time and viscosity were found to be 1.65 min, 1.59 min, 1607.9 Pa. s, and 1595 Pa.s, respectively. Each independent variable checkpoint formulation was developed in triplicate. It was discovered that the experimental values of the batch that was ultimately prepared were quite similar to the expected value. All parameters in the model were successfully validated with a 95% confidence level.

In-situ mucoadhesive gel Preparation

According to Gomathi et al., chitosan was soluble at the desired concentration (0.5% w/v) in an acetate buffer with a pH of 4.6 [51]. The ability of the aqueous solution of Carbopol to change into a firm gel upon increasing the pH supports the implementation of in situ gelling devices [35]. However, the higher quantity of

Carbopol is essential to generate a firm gel thus resulting in very acidic solutions. Hence, it is difficult for the throat mucosa to neutralize this acidic solution. The employment of viscosity-improving polymers like chitosan resulted in the opportunity to reduce Carbopol content without affecting the delivery system's capability to gel and its rheological characteristics. Formulation with optimized Carbopol concentration (0.3%) and chitosan concentration (0.5%) retained their liquid states (clear solutions) at room temperature and at the pH that was formulated, and they both exhibited good gelling strength at pH 6.7. The solution and gelling state of the optimized in-situ gel formulation in Fig. 5a.

Characterization of the optimized in-situ mucoadhesive gel

General appearance

The formulation appearance and transparency were visually analyzed under fluorescent lighting, alternately against white and black backdrops. The formulation was observed to be elegant and transparent, with the absence of any particulate matter. Due to chitosan's solubility in acidic conditions, its odor was slightly pungent, improved by the addition of carbopol. The polymeric mixture of mucoadhesive scaffold used at the concentration evaluated has no gritty texture.

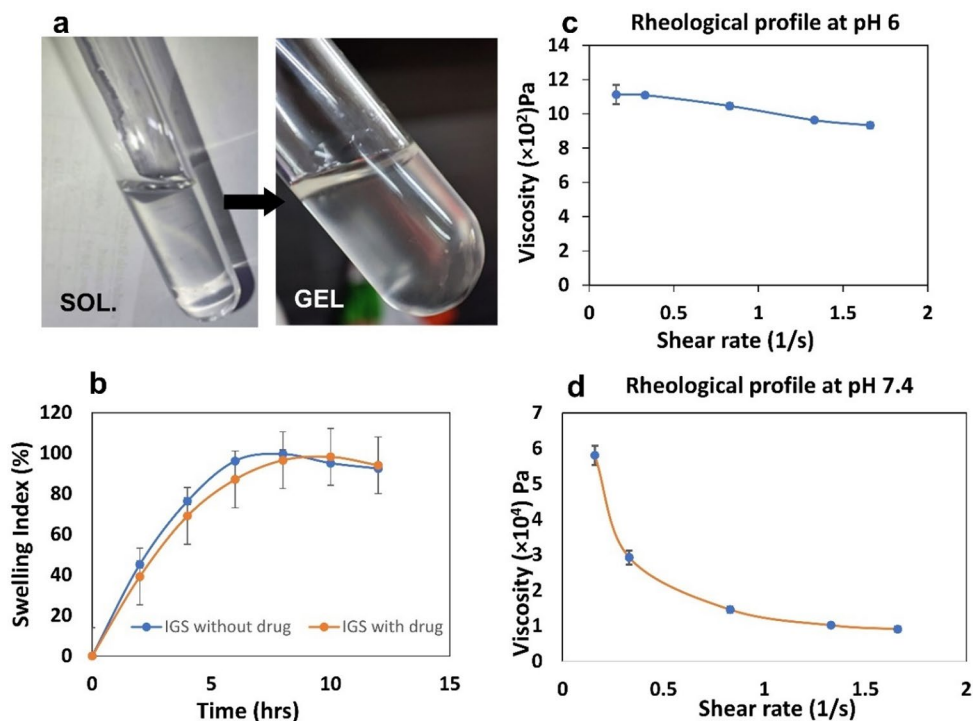


Fig. 5 Sol to gel conversion, rheological study, and swelling index of prepared formulation. (a) Optimized in-situ gel formulation, (b) Swelling properties of optimized gel with drug and without drug, (c&d) Rheological properties of the optimized formulation

Determination of gelation pH

The pH of the optimized pH-sensitive polymeric solution was 5.9 ± 0.3 . Upon increasing the pH of this solution to about 7.0, it was successfully converted into a gel. This confirms the pH-sensitive behavior of the polymer [52]. Therefore, the polymer solution can be expected to transform into a gel when administered into the upper respiratory tract due to the physiological pH of the throat [53]. The pH was measured after gel formation, which was found to be 7.2 ± 0.2 . This seems compatible with delivery to the throat as the throat mucosa wouldn't be irritated.

Rheological studies

The amount of gel adhering to the throat mucosa in the local drug delivery system might be dropped. Therefore, increasing viscosity is essential for effective retention and improved therapeutic response at the site of action [54]. This indicates that the gel has a shear-thinning tendency, which means it becomes easier to spread or move when shear stress is applied, such as the force of swallowing. Additionally, it is crucial that the patient does not feel irritated; therefore, the viscosity must be ideal. The formulation had low viscosity and was liquid at pH 6.0. Upon increasing the pH to 7.4, the liquid or solution state changed into a highly viscous gel. Hence, the formulation's performance depends on its capacity to change at physiological pH from a liquid to a gel as well as on its pseudoplastic rheological characteristics. The optimized formulation underwent shear thinning, and when shear stress increased, angular velocity increased as well (pseudoplastic rheology) as shown in Fig. 5c and d.

Spreadability

According to the spreadability data, the gel formulation demonstrated excellent spreading ability under applied shear, a critical component for patient comfort and convenience of drug delivery systems [55]. The results also showed that the polymeric components were viscoelastic since they all had established mucoadhesive properties. These components allow the gel to adhere firmly to the throat mucosa, ensuring long-term retention at the intended location. In general, the fabricated scaffold displayed good homogeneity and was lump-free, indicating uniform drug distribution within the gel. The optimized formulation exhibits a good spreadability index of $322.6 \pm 0.5\%$. It signifies that the gel's high spreadability under moderate pressure enhances its ease of use and therapeutic efficacy [56]. It covers a large area of the mucosal surface with a small amount, improving drug performance without excessive formulation. Its favorable spreadability, viscoelasticity, and homogeneity make it suitable for mucosal applications.

Matrix erosion

In drug delivery systems, erosion plays a crucial role because it affects the drug's release and clearance, particularly in local applications on mucosal surfaces [57]. High values have been identified for the formulation regarding erosion of the gel formulation. In the case of the optimized gel formulation, more than $98\% \pm 1.6$ ($n=3$) of the erosion was observed after 24 h indicate that the formulation is designed to degrade or dissolve at a controlled rate over time. The high percentage of erosion also indicates that the gel has dissolved by the end of the 24-hour period, which is advantageous in preventing the formulation from building up or causing discomfort once its therapeutic effect has been attained.

Swelling index

The two generated formulations of the optimized gel system initially offered a boost in the swelling index values. In comparison to the drug-containing formulation, the drug-free formulation exhibits a better swelling index, as represented in the graph (Fig. 5b). This suggests that the presence of the drug may slightly hinder the gel's ability to absorb fluid and swell [58]. The in-situ gel system without the drug exhibits a spike in the swelling index for the first 8 ($99.6 \pm 0.09\%$) hours before declining throughout the next 12 h. Similarly to the drug-infused in-situ gel approach, the swelling index increases for the first 10 ($98.26 \pm 1.54\%$) hours before declining over the next 12 h. It may be caused by drug molecules becoming trapped in the gel system's void space. As the gel swells, it absorbs fluids, which can help solubilize and release the drug over time. Additionally, it shows that the gel expanded and absorbed fluid quickly in the early hours, which is advantageous for an immediate initial effect, such as developing strong mucoadhesion [59].

Ex vivo mucoadhesive strength

It is important to analyze the adhesion of gel to the throat mucus membrane as a longer residence time of the formulation is desired for improved therapeutic effect [60]. Otherwise, mucoadhesive strength reflects the retention ability of the developed in-situ gel. If the mucoadhesive strength of the formulation is higher, there are more chances of preventing its clearance from the upper respiratory tract. It will be more retained in the targeted area if the drug delivery system has high mucoadhesiveness. This will further enhance the drug permeation rate through epithelial layers of the mucosa; therefore, the desired drug concentration can be attained at the target site [61]. In the developed in situ gel, the presence of polymers like chitosan and carbopol imparted mucoadhesiveness [62]. Chitosan, being a cationic polymer, binds to the negatively charged mucus and has been extensively exploited for developing mucoadhesive drug delivery

systems [63]. Crosslinked carbopol has numerous carboxylic groups that bind to the sugar residues present in mucus through hydrogen bonding [62]. From the experiment, the mucoadhesive detachment force of the prepared formulation was observed to be 589 g/cm^2 which reflects the high mucoadhesive strength of the developed formulation (Fig. 6a). This value indicates that the gel may withstand external forces that cause it to separate, including swallowing or throat movement, allowing for a longer period of residence. In a similar study, Nair et al. developed a darunavir-loaded mucoadhesive in situ gel composed of poloxamer and carbopol which exhibited good mucoadhesive strength [64].

In-vitro drug release

The in vitro drug release study of the optimized in-situ gel system was performed via the dialysis bag method in dissolution media of PBS (pH 7.4) for 12 h and compared to the release pattern showed by the pure drug. A graph (Fig. 6b) was plotted showing the cumulative percent

drug release versus time for two samples, with time in hours on the x-axis and % cumulative drug release on the y-axis. According to in vitro studies, the total amount of drug released from the in-situ gel after 12 h was 1.4-fold higher compared to pure drug. This could be attributed to the improvement in drug solubility due to the formation of the inclusion complex of ATM [65, 66]. About 75% of ATM was released from the in-situ gel in 6 h, after which a sustained release till 12 h was observed. The release behavior of Azithromycin (ATM) and its HP- β CD inclusion complex from the gel matrix revealed a dual-phase pattern (Fig. 6b). Initially, both free ATM and the inclusion complex exhibited a similar release profile up to 5 h. This can be attributed to the release of drug molecules loosely associated with the surface or near-surface layers of the gel matrix. Despite the higher solubility of the inclusion complex (as evidenced in Fig. 3), the early release phase is governed more by surface kinetics than solubility enhancement.

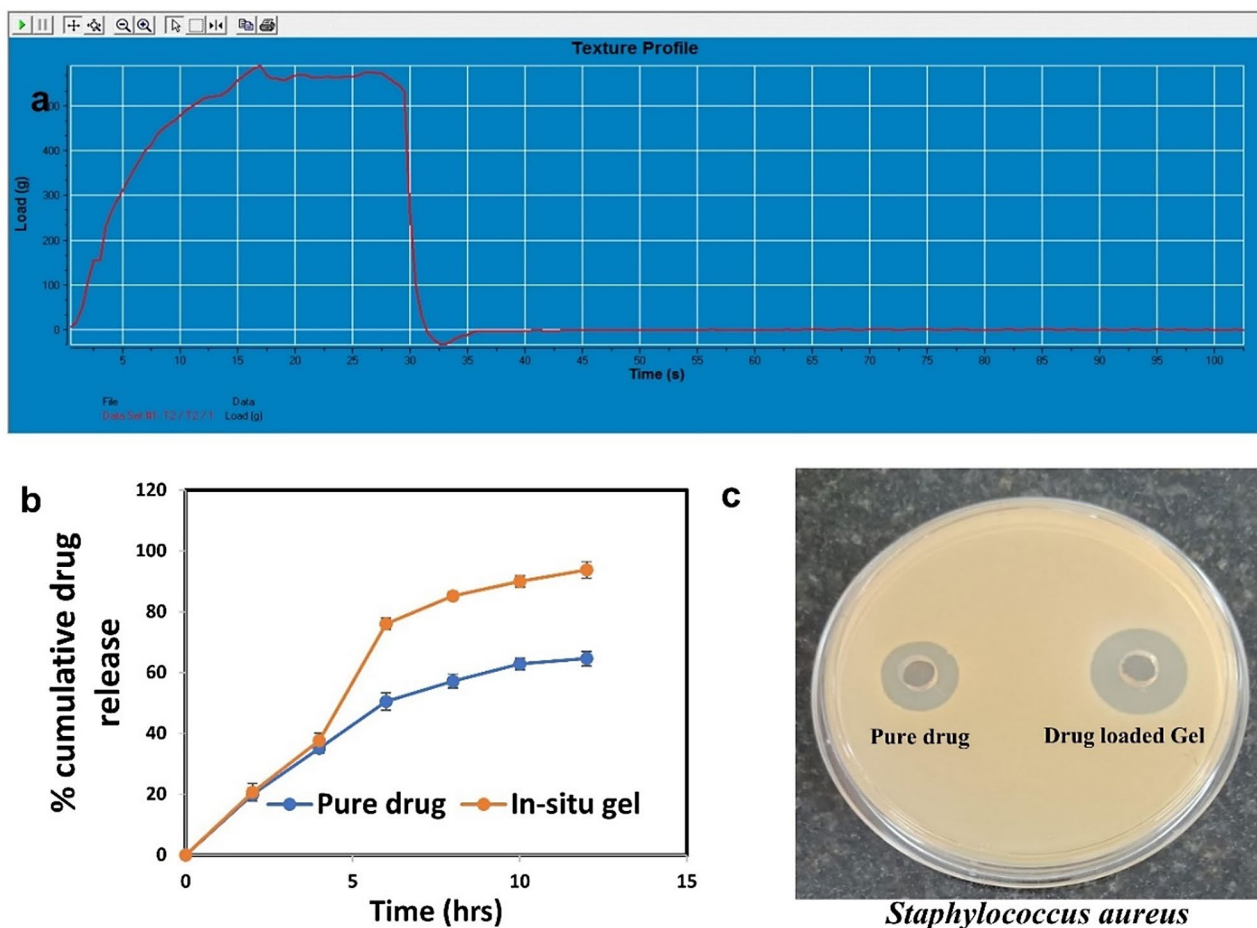


Fig. 6 Texture analysis of prepared in situ gel to study mucoadhesive detachment force, cumulative drug release profile and antimicrobial profile of Azithromycin loaded in situ gel. **(a)** Mucoadhesive strength of in situ gel, **(b)** In-vitro drug release profile of Azithromycin from in situ gel, **(c)** Antimicrobial activity utilizing agar well diffusion method against *Staphylococcus aureus* bacterial cultures representing the zone of inhibition surrounding the wells containing pure drug and drug-loaded in situ gel

Table 4 Antibacterial properties by agar well diffusion method
Zone of Inhibition in (mm)

Formulations	<i>Staphylococcus aureus</i> zone of inhibition (Mean \pm SD, $n=3$) and MIC			
	12 h	24 h	48 h	MIC
Azithromycin	11 \pm 1.31 mm	15 \pm 1.12 mm	19 \pm 1.27 mm	3 μ g/ mL
In-situ gel	18 \pm 2.16 mm	28 \pm 2.05 mm	31 \pm 3.54 mm	1 μ g/ mL

However, beyond 5 h, the inclusion complex exhibited a significantly higher release compared to free ATM. This shift is attributed to the superior aqueous solubility of the HP- β CD complex, which enhances drug diffusion through the rigid gel matrix formed by electrostatic interactions between carbopol and chitosan. In contrast, the poor solubility of free ATM becomes a limiting factor in its sustained release phase. The findings collectively indicate that although the gel formulation imparts a controlled release profile, the solubility advantage of the inclusion complex facilitates higher drug availability in the latter phase of the release timeline [67]. In a study, darunavir-loaded mucoadhesive in situ gel was developed for intranasal delivery, where about 95% of the drug was released in 8 h [64]. Further, the drug release kinetic data of ATM best fit into the Regression coefficient (R2) for Korsmeyer-Peppas's model was 0.9344. By examining the drug release pattern from the polymeric system, the in vitro release data of this layer were fitted using Korsmeyer-Peppas's equation. "With a value of 0.61 for "n," it was discovered that the drug release is consistent with super case-I transport, or the Fickian model. Diffusion controlled drug release in this model. When compared to the polymeric chain relaxing process, the solvent transport rate or diffusion is substantially higher".

In-vitro antimicrobial activity

As shown in Table 4, the zones of growth inhibition (mm) of *Staphylococcus aureus* were tested and compared for test formulations, i.e., situ gel of ATM HP- β -cyclodextrin complex (Fig. 6c). In-situ gel portrayed an enhanced growth inhibition zone because of its controlled drug release, improve ATM solubility and diffusion surrounding the microbial growth medium. In particular, the in-situ gel formulation enabled sustained and gradual release of ATM, maintaining an effective drug concentration over time to inhibit bacterial growth. Incorporating the HP- β -cyclodextrin complex significantly improved ATM's solubility and bioavailability, allowing for better diffusion into the surrounding medium [68, 69]. This investigation implied that the in-situ gel of ATM cyclodextrin complex has antimicrobial efficacy against *Staphylococcus aureus*.

Table 5 In-vivo antimicrobial assay of the in-situ gel against
Staphylococcus aureus

Colony forming units (CFU)/mL			
After disease induction	Time	After treatment	
		Developed formulation	Marketed formulation
13.21 \pm 2.48 $\times 10^2$	24	1.36 \pm 0.34 $\times 10^2$	1.24 \pm 0.49 $\times 10^2$
	48	0.64 \pm 0.08 $\times 10^2$	0.93 \pm 0.62 $\times 10^2$

MIC determination

After 24 h of incubation at 37 °C under aerobic conditions, a reduction in turbidity was observed in the test tubes containing 1 μ g/mL of ATM for the formulation and 3 μ g/mL for the free drug, indicating bacterial growth inhibition. No turbidity was detected at the 5 μ g/mL concentration, indicating complete inhibition of bacterial growth. It means formulation antimicrobial efficacy is more significant than the free drug. Again, this may be due to the solubility enhancement of the antimicrobial activity of ATM, mainly through solubility improvements, and for the in-situ gel formulation, which is more effective than the free drug in inhibiting bacterial growth at lower concentrations. Antimicrobial effects are typically evaluated using agar diffusion and MIC tests. The advantage of direct contact tests over the agar diffusion method is that they are not dependent on the diffusion properties of the tested material and media. Serial dilutions are employed in MIC testing to determine the lowest concentration of a substance that still exhibits antibacterial activity [70].

In-vivo characterization of the in-situ gel

Antimicrobial study

In the in-vivo antimicrobial study, ATM in-situ gel were compared with and marketed ATM formulations, as shown in Table 5. The antimicrobial efficacy of the developed formulation was determined by comparing the reduction in CFU counts after i.v. administration of formulations to disease-induced albino rats. Results of in-vivo activity demonstrated that the developed formulation showed higher activity than the marketed formulation. This could be attributed to the higher residence time of the developed formulation at the site of action. This could relate to the developed formulation's improved drug solubility and mucoadhesive behaviour, which helps to escape the formulation from fast-pass metabolism. Control drug release further ensures the optimum quantity of drugs available in the site of action [71].

In vivo retention and bio-analytical Estimation

The mucoadhesive properties of the developed formulation aim to enhance drug retention at the targeted mucosal site. The retention efficacy of the optimized formulation was evaluated in rats using radiographic

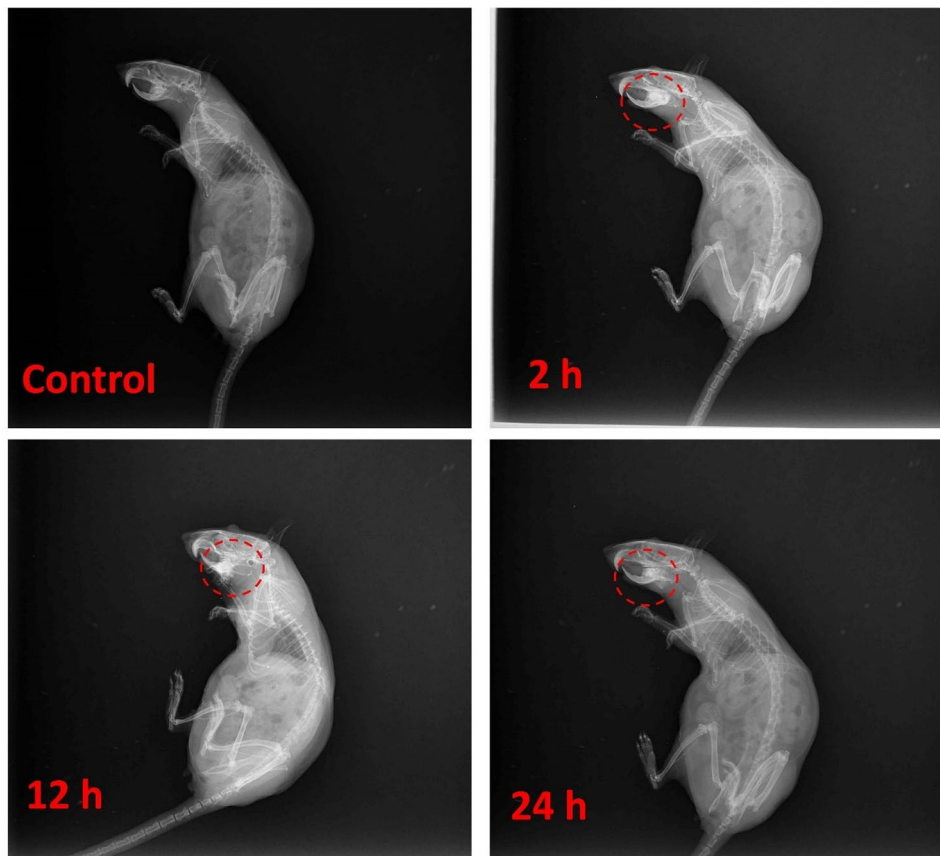


Fig. 7 X-ray images of animals administered with the placebo and the in situ gel formulation at 2, 12, and 24 h

imaging. Figure 7 presents X-ray images of animals administered with the placebo and the in situ gel formulation at 2, 12, and 24 h during the study. The in situ gel, containing barium sulfate as a contrast agent, was utilized to assess the formulation's retention time. The results indicate that the mucoadhesive formulation remained in the throat for an extended period (24 h). X-ray analysis further confirmed the formulation's retention in the throat region. Additionally, bioanalytical studies revealed that approximately $21 \pm 0.26\%$ of the drug remained at the application site after 12 h and $02 \pm 0.01\%$ after 24 h of administration. Prolonged retention in the throat region could improve efficacy against upper respiratory tract infections (URTIs), commonly observed during the rainy and winter seasons.

Conclusion

Haemophilus influenzae, *Staphylococcus pneumoniae*, *Staphylococcus aureus*, and *Chlamydia pneumoniae* are some prevalent bacteria that cause URTIs and sore throats. The broad use of ATM to treat URTIs is limited by its poor oral absorption and gastrointestinal adverse effects. These issues can be resolved through the development of a formulation that is site-specific. An HP- β CD inclusion complex-based in situ pH-responsive

mucoadhesive gel of ATM was prepared to overcome these issues. The inclusion complex of ATM with HP- β CD improves the solubility of ATM by 20-fold. The optimized formulation was found to have a higher drug load, optimum gelation time and viscosity at the desired pH range. It transitions from liquid to gel at pH 7.4, enhancing retention. The formulation exhibits a good mucoadhesive strength of 589 g/cm^2 and improved drug release compared to pure ATM. Furthermore, it displays a wider zone of *Staphylococcus aureus* growth inhibition ($31 \pm 3.54 \text{ mm}$) and a sustained drug release profile for 12 h (94%). The developed mucoadhesive in situ gels demonstrated promising in vivo performance, primarily due to their effective antimicrobial activity. In vivo, local retention studies confirmed that the formulations adhered to the throat mucosa and remained in place for up to 24 h after application. Also, the formation of an inclusion complex with HP- β CD can provide better stability and solubility. According to the results shown here, this localised delivery method could effectively increase ATM's therapeutic effectiveness against URTIs.

Acknowledgements

The authors acknowledge the Researchers Supporting Project number (RSPD2025R708), King Saud University, Riyadh, Saudi Arabia, for funding this

research work. The authors also acknowledge the financial support of the Department of Biotechnology (DBT), Govt. India.

Author contributions

J.H.: data collection, experimental work, compilation, and manuscript writing. S.M., R.M. M.T. and D.P.: data collection and experimental work. A.M, I.S.: compilation and manuscript writing. V.K.R. and R.K.S: data analysis, language editing, and critical analysis. B.K.: animal experiment and data interpretation. G.G.: conceptualization of the topics and critical analysis. G.R.: conceptualization of the topic and design of the table of content, data analysis, and paper writing, editing, and proof reading.

Funding

Open access funding provided by Siksha 'O' Anusandhan (Deemed To Be University)

This work was supported by the Department of Biotechnology (DBT), Government of India, under the DBT Builder project with order no BT/INF/22/SP45078/2022.

Data availability

No datasets were generated or analysed during the current study.

Declarations

Consent for publication

All the authors involved in this study gave permission for their experimental findings involved in this research study to be published in a research paper.

Competing interests

The authors declare no competing interests.

Author details

¹School of Pharmaceutical Sciences, Siksha O Anusandhan (Deemed to be University), Bhubaneswar, Odisha, India

²Department of Botany and Microbiology, College of Science, King Saud University, P.O. Box. 2454, Riyadh 11451, Saudi Arabia

³Department of Biotech and Biomolecular Science, University of New South Wales, Sydney, NSW 2033, Australia

⁴Department of Pharmaceutics, School of Pharmaceutical Science, Siksha 'O' Anusandhan (Deemed to be University), Bhubaneswar, Odisha 751003, India

Received: 19 February 2025 / Accepted: 25 April 2025

Published online: 29 April 2025

References

- Tang J, et al. Diversity of upper respiratory tract infections and prevalence of *Streptococcus pneumoniae* colonization among patients with fever and flu-like symptoms. *BMC Infect Dis*. 2019 Dec;19(1):24. <https://doi.org/10.1186/s12879-018-3662-z>.
- Donde S, Mishra A, Kochhar P. Azithromycin in acute bacterial upper respiratory tract infections: An Indian non-interventional study. *Indian J Otolaryngol Head Neck Surg*. 2014 Jan;66(S1):225–30. <https://doi.org/10.1007/s12070-011-0437-x>.
- Jain N, Lodha R, Kabra SK. Upper respiratory tract infections. *Indian J Pediatr*. 2001 Dec;68(12):1135–1138. <https://doi.org/10.1007/BF02722930>
- Windfuhr JP, Toepfner N, Steffen G, Waldfahrer F, Berner R. Clinical practice guideline: tonsillitis I. Diagnostics and nonsurgical management. *Eur Arch Otorhinolaryngol*. 2016 Apr;273(4):973–87. <https://doi.org/10.1007/s00405-015-3872-6>.
- Jama-Kmiecik A, Frej-Mądrzak M, Sarowska J, Choroszy-Król I. Pathogens causing upper respiratory tract infections in outpatients. In: Pokorski M, editor. Pulmonary dysfunction and disease. Advances in experimental medicine and biology. Cham: Springer International Publishing; 2016:934:89–93. https://doi.org/10.1007/5584_2016_19
- Kanwal S, Vaitla P. *Streptococcus Pyogenes*. In StatPearls. Treasure Island (FL): StatPearls Publishing; 2024. Accessed: May 17, 2024. [Online]. Available: <http://www.ncbi.nlm.nih.gov/books/NBK554528/>
- Bhattacharya S. The facts about penicillin allergy: a review. *J Adv Pharm Technol Res*. 2010 Jan;1(1):11–17
- Alvarez-Elcoro S, Enzler MJ. The Macrolides: erythromycin, clarithromycin, and azithromycin. *Mayo Clin Proc*. 1999 Jun;74(6):613–634. <https://doi.org/10.4065/74.6.613>
- Singlas E. Clinical pharmacokinetics of azithromycin. *Pathol Biol (Paris)*. 1995 Jun;43(6):505–511.
- Boelig RC, Lam E, Rochani A, Kaushal G, Roman A, Kraft WK. Longitudinal evaluation of azithromycin and cytokine concentrations in amniotic fluid following one-time oral dosing in pregnancy. *Clin Transl Sci*. 2021 Nov;14(6):2431–2439. <https://doi.org/10.1111/cts.13111>
- Ulbricht C, Chao W, Costa D, Rusie-Seamon E, Weissner W, Woods J. Clinical Evidence of herb-drug interactions: A systematic review by the Natural Standard Research Collaboration. *Curr Drug Metab*. 2008 Dec;9(10):1063–1120. <https://doi.org/10.2174/138920008786927785>
- Bryskier A, Bergogne-Bérézin E. Macrolides. In: Bryskier A, editor. Antimicrobial agents. Washington, DC, USA: ASM Press; 2014:475–526. <https://doi.org/10.1111/97811555815929.ch18>
- Ventola CL. The antibiotic resistance crisis: part 1: causes and threats. *PT Peer-Rev J Formul Manag*. 2015 Apr;40(4):277–283.
- Mishra B, Singh J. Novel drug delivery systems and significance in respiratory diseases. In Targeting chronic inflammatory lung diseases using advanced drug delivery systems. Elsevier; 2020:57–95. <https://doi.org/10.1016/B978-0-12-820658-4.00004-2>.
- Saha I, et al. Novel drug delivery approaches for the localized treatment of cervical Cancer. *AAPS PharmSciTech*. 2024 Apr;25(4):85. <https://doi.org/10.1208/s12249-024-02801-1>.
- Firth A, Prathapan P. Azithromycin: the first broad-spectrum therapeutic. *Eur J Med Chem*. 2020 Dec;207:112739. <https://doi.org/10.1016/j.ejmech.2020.112739>.
- Douafer H, Andrieu V, Brunel JM. Scope and limitations on aerosol drug delivery for the treatment of infectious respiratory diseases. *J Controlled Release*. 2020 Sep;325:276–292. <https://doi.org/10.1016/j.jconrel.2020.07.002>
- Taylor G, Gumbleton M. Aerosols for macromolecule delivery: design challenges and solutions. *Am J Drug Deliv*. 2004;2(3):143–55. <https://doi.org/10.2165/00137696-200402030-00001>.
- Cao F, Zhang X, Ping Q. New method for ophthalmic delivery of azithromycin by poloxamer/carbopol-based in situ gelling system. *Drug Deliv*. 2010 Oct;17(7):500–507. <https://doi.org/10.3109/10717544.2010.483255>
- Sharma M, Deohra A, Reddy KR, Sadhu V. Biocompatible in-situ gelling polymer hydrogels for treating ocular infection. In: *Methods in Microbiology*. Elsevier; 2019;46:93–114. <https://doi.org/10.1016/bs.mim.2019.01.001>.
- Li J, et al. Preparation of azithromycin amorphous solid dispersion by hot-melt extrusion: An advantageous technology with taste masking and solubilization effects. *Polymers*. 2022 Jan;14(3):495. <https://doi.org/10.3390/polym14030495>.
- Amin F, et al. A new strategy for taste masking of azithromycin antibiotic: development, characterization, and evaluation of azithromycin titanium nanohybrid for masking of bitter taste using physisorption and panel testing studies. *Drug Des Devel Ther*. 2018 Nov;12:3855–3866. <https://doi.org/10.2147/DDDT.S183534>
- Chauhan R, Madan J, Kaushik D, Sardana S, Pandey RS, Sharma R. Inclusion complex of colchicine in hydroxypropyl- β -cyclodextrin tenders better solubility and improved pharmacokinetics. *Pharm Dev Technol*. 2013 Apr;18(2):313–322. <https://doi.org/10.3109/10837450.2011.591801>
- Bhimani S, et al. Development of the UV spectrophotometric method of azithromycin in API and stress degradation studies. *Int Lett Chem Phys Astron*. 2016 Jul;68:48–53. <https://doi.org/10.56431/p-z2wv9>.
- Ghari T, Kobarfard F, Mortazavi SA. Development of a simple RP-HPLC-UV method for determination of azithromycin in bulk and pharmaceutical dosage forms as an alternative to the USP method. *Iran J Pharm Res IJPR*. 2013;12(Suppl):57–63.
- Doile MM, Fortunato KA, Schmücker IC, Schucko SK, Silva MAS, Rodrigues PO. Physicochemical properties and dissolution studies of dexamethasone acetate-beta-cyclodextrin inclusion complexes produced by different methods. *AAPS PharmSciTech*. 2008;9(1):314–21. <https://doi.org/10.1208/s12249-008-9042-z>.
- Loh GOK, Tan YTF, Peh K-K. Enhancement of norfloxacin solubility via inclusion complexation with β -cyclodextrin and its derivative hydroxypropyl- β -cyclodextrin. *Asian J Pharm Sci*. 2016 Aug;11(4):536–46. <https://doi.org/10.1016/j.ajps.2016.02.009>.

28. Raval M, Bagada H. Formulation and evaluation of cyclodextrin-based thermosensitive in situ gel of azithromycin for periodontal delivery. *J Pharm Innov.* 2021;16(1):67–84. <https://doi.org/10.1007/s12247-019-09422-3>
29. Ridhurkar DN, et al. Inclusion complex of aprepitant with cyclodextrin: evaluation of physico-chemical and pharmacokinetic properties. *Drug Dev Ind Pharm.* 2013;39(11):1783–1792. <https://doi.org/10.3109/03639045.2012.737331>
30. Aigner Z, Berkesi O, Farkas G, Szabó-Révész P. DSC, X-ray and FTIR studies of a gemfibrozil/dimethyl- β -cyclodextrin inclusion complex produced by co-grinding. *J Pharm Biomed Anal.* 2012 Jan;57:62–7. <https://doi.org/10.1016/j.jpba.2011.08.034>
31. Marques H, Hadgraft J, Kellaway I. Studies of cyclodextrin inclusion complexes. I. The salbutamol-cyclodextrin complex as studied by phase solubility and DSC. *Int J Pharm.* 1990 Sep;63(3):259–66. [https://doi.org/10.1016/0378-5173\(90\)90132-N](https://doi.org/10.1016/0378-5173(90)90132-N)
32. Aytac Z, Kusku SI, Durgun E, Uyar T. Quercetin/ β -cyclodextrin inclusion complex embedded nanofibres: Slow release and high solubility. *Food Chem.* 2016 Apr;197:864–71. <https://doi.org/10.1016/j.foodchem.2015.11.051>
33. Dua K, Pabreja K, Ramana M, Lather V. Dissolution behavior of β -cyclodextrin molecular inclusion complexes of aceclofenac. *J Pharm Bioallied Sci.* 2011;3(3):417. <https://doi.org/10.4103/0975-7406.84457>
34. Halder J, et al. Glycyrrhizin loaded hyaluronic acid nanofiber-based artificial saliva for the management of oral mucositis: Preparation, optimization and in-vitro evaluation. *J Drug Deliv Sci Technol.* Sep. 2023;87:104777. <https://doi.org/10.1016/j.jddst.2023.104777>
35. Saha I, Palak A, Rai VK. Relevance of NLC-gel and microneedling-assisted tacrolimus ointment against severe psoriasisiform: In vitro dermal retention kinetics, in vivo activity and drug distribution. *J Drug Deliv Sci Technol.* 2022 May;71:103272. <https://doi.org/10.1016/j.jddst.2022.103272>
36. Rai VK, et al. Development of cellulosic polymer based gel of novel ternary mixture of miconazole nitrate for buccal delivery. *Carbohydr Polym.* 2014;103:126–133. <https://doi.org/10.1016/j.carbpol.2013.12.019>
37. Hani U, et al. 23 Full factorial design for formulation and evaluation of floating oral in situ gelling system of piroxicam. *J Pharm Innov.* 2021;16(3):528–536. <https://doi.org/10.1007/s12247-020-09471-z>
38. Joshi N, Mishra N, Rai VK. Development and evaluation of in situ gel of silver sulfadiazine for improved therapeutic efficacy against infectious burn wound. *J Pharm Innov.* 2021;16(3):537–550. <https://doi.org/10.1007/s12247-020-09464-y>
39. Garala K, Joshi P, Shah M, Ramkishan A, Patel J. Formulation and evaluation of periodontal in situ gel. *Int J Pharm Investig.* Jan. 2013;3(1):29–41. <https://doi.org/10.4103/2230-973X.108961>
40. Chaudhary SC. Formulation & evaluation of floatable insitu gel for stomach-specific drug delivery of ofloxacin. *Am J Adv Drug Deliv.* 2013;1(3):285–99.
41. Patel N, Baldaniya M, Raval M, Sheth N. Formulation and development of in situ nasal gelling systems for quetiapine fumarate-loaded mucoadhesive microemulsion. *J Pharm Innov.* 2015;10(4):357–373. <https://doi.org/10.1007/s12247-015-9232-7>
42. Alimohammadi SD. Preparation and in vivo evaluation of in situ gel system as dual thermo-/pH-responsive nanocarriers for sustained ocular drug delivery. *J Microencapsul.* 2015 Jul;32(5):511–9. <https://doi.org/10.3109/02652048.2015.1065915>
43. Polat HK, et al. Formulation development of dual drug-loaded thermo-sensitive ocular in situ gel using factorial design. *J Pharm Innov.* 2023 Jun;18(2):768–88. <https://doi.org/10.1007/s12247-023-09762-1>
44. Das MC, Biswas A, Chowdhury M, Saha J. Screening antimicrobial susceptibility of gentamicin, vancomycin, azithromycin, chloramphenicol and cefotaxime against selected gram positive and gram negative bacteria. *Int J Pharma Res Health Sci.* 2014;2(4):324–331.
45. Rai VK, et al. Spray-dried mucoadhesive re-dispersible gargle of chlorhexidine for improved response against throat infection: Formulation development, in vitro and in vivo evaluation. *AAPS PharmSciTech.* 2024 Feb;25(2):31. <https://doi.org/10.1208/s12249-024-02750-9>
46. Colley HE, et al. Pre-clinical evaluation of novel mucoadhesive bilayer patches for local delivery of clobetasol-17-propionate to the oral mucosa. *Biomaterials.* 2018 Sep;178:134–46. <https://doi.org/10.1016/j.biomaterials.2018.06.009>
47. Shah SS, Pasha TY, Behera AK, Bhandari A. Solubility enhancement and physicochemical characterization of inclusion complexes of itraconazole. *Pharm Lett.* 2012;4(1):354–366.
48. Lu N, Xu H, Liu Y. Characterization and antimicrobial activity of a 2-O-methyl- β -cyclodextrin inclusion complex containing hexahydro- β -acids. *J Mater Sci.* 2019 Mar;54(5):4287–4296. <https://doi.org/10.1007/s10853-018-3148-9>
49. Manne ASN, Hegde AR, Raut SY, Rao RR, Kulkarni VI, Mutalik S. Hot liquid extrusion assisted drug-cyclodextrin complexation: A novel continuous manufacturing method for solubility and bioavailability enhancement of drugs. *Drug Deliv Transl Res.* 2021 Jun;11(3):1273–1287. <https://doi.org/10.1007/s13346-020-00854-w>
50. Shanmuga Priya A, Sivakamavalli J, Vaseeharan B, Stalin T. Improvement on dissolution rate of inclusion complex of rifabutin drug with β -cyclodextrin. *Int J Biol Macromol.* 2013 Nov;62:472–480. <https://doi.org/10.1016/j.jbiomac.2013.09.006>
51. Gomathi T, Sudha PN, Florence JAK, Venkatesan J, Anil S. Fabrication of letrozole formulation using chitosan nanoparticles through ionic gelation method. *Int J Biol Macromol.* 2017 Nov;104:1820–32. <https://doi.org/10.1016/j.jbiomac.2017.01.147>
52. Yadav N, Parashar AK, Sethi VA. Development and Assessment of In-Situ Gel Formulation for Ocular Pain and Inflammation. *Int J Newgen Res Pharm Healthc.* 2024 Jun;2(1):248–54. <https://doi.org/10.61554/ijnrph.v2i1.2024.71>
53. Fabricant ND. Introduction to the pH of the Throat. *Arch Otolaryngol - Head Neck Surg.* 1943 Feb;37(2):169–73. <https://doi.org/10.1001/archotol.1943.00670030178002>
54. Gratieri T, Gelfuso GM, Rocha EM, Sarmento VH, De Freitas O, Lopez RFV. A poloxamer/chitosan in situ forming gel with prolonged retention time for ocular delivery. *Eur J Pharm Biopharm.* 2010 Jun;75(2):186–93. <https://doi.org/10.1016/j.ejpb.2010.02.011>
55. Shahin M, Abdel Hady S, Hammad M, Mortada N. Novel jojoba oil-based emulsion gel formulations for clotrimazole delivery. *AAPS PharmSciTech.* 2011 Mar;12(1):239–47. <https://doi.org/10.1208/s12249-011-9583-4>
56. Kumbhar D, Wavikar P, Vavia P. Niosomal gel of lornoxicam for topical delivery: in vitro assessment and pharmacodynamic activity. *AAPS PharmSciTech.* 2013 Sep;14(3):1072–82. <https://doi.org/10.1208/s12249-013-9986-5>
57. Sankar V, et al. Local drug delivery for oral mucosal diseases: challenges and opportunities. *Oral Dis.* 2011 Apr;17(5):73–84. <https://doi.org/10.1111/j.1601-0825.2011.01793.x>
58. Kim SW, Bae YH, Okano T. Hydrogels: Swelling, drug loading, and release. *Pharm Res.* 1992;9(3):283–90. <https://doi.org/10.1023/A:1015887213431>
59. Almeida H, Amaral MH, Lobão P, Lobo JMS. In situ gelling systems: a strategy to improve the bioavailability of ophthalmic pharmaceutical formulations. *Drug Discov Today.* 2014 Apr;19(4):400–12. <https://doi.org/10.1016/j.drudis.2013.10.001>
60. Belgamwar VS, Chauk DS, Mahajan HS, Jain SA, Gattani SG, Surana SJ. Formulation and evaluation of in situ gelling system of dimenhydrinate for nasal administration. *Pharm Dev Technol.* 2009 Jun;14(3):240–8. <https://doi.org/10.1080/10837450802498910>
61. Garg A, Garg S, Pandey P, Madamsetty VS, Mishra N. Mucoadhesive drug delivery system in chronic respiratory diseases. In: Chellappan DK, Pabreja K, Md, Faiyazuddin, editors. *Advanced drug delivery strategies for targeting chronic inflammatory lung diseases.* Singapore: Springer Singapore; 2022:435–69. https://doi.org/10.1007/978-981-16-4392-7_19
62. Shelke S, Shahi S, Jalalpure S, Dhamecha D, Shengule S. Formulation and evaluation of thermoreversible mucoadhesive in-situ gel for intranasal delivery of naratriptan hydrochloride. *J Drug Deliv Sci Technol.* 2015 Oct;29:238–244. <https://doi.org/10.1016/j.jddst.2015.08.003>
63. Andersen T, Bleher S, Eide Flaten G, Tho I, Mattsson S, Škalko-Basnet N. Chitosan in Mucoadhesive Drug Delivery: Focus on Local Vaginal Therapy. *Mar Drugs.* 2015 Jan;13(1):222–236. <https://doi.org/10.3390/md13010222>
64. Nair AB, et al. Intranasal delivery of darunavir-loaded mucoadhesive in situ gel: Experimental design, in vitro evaluation, and pharmacokinetic studies. *Gels.* 2022 May;8(6):342. <https://doi.org/10.3390/gels8060342>
65. Rawat S, Jain SK. Solubility enhancement of celecoxib using β -cyclodextrin inclusion complexes. *Eur J Pharm Biopharm.* 2004 Mar;57(2):263–7. <https://doi.org/10.1016/j.ejpb.2003.10.020>
66. Sid D, et al. Solubility enhancement of mefenamic acid by inclusion complex with β -cyclodextrin: in silico modelling, formulation, characterisation, and in vitro studies. *J Enzyme Inhib Med Chem.* 2021 Jan;36(1):605–17. <https://doi.org/10.1080/14756366.2020.1869225>
67. Gupta S. Carbopol/Chitosan based pH triggered in situ gelling system for ocular delivery of timolol maleate. *Sci Pharm.* 2010;78(4):959–76. <https://doi.org/10.3797/scipharm.1001-06>
68. Thakkar HP, Khunt A, Dhande RD, Patel AA. Formulation and evaluation of Itraconazole nanoemulsion for enhanced oral bioavailability. *J Microencapsul.* 2015 Aug;32(6):559–69. <https://doi.org/10.3109/02652048.2015.1065917>
69. Pimple P, Singh P, Prabhu A, Gupta S. Development and optimization of HP- β -CD inclusion complex-based fast orally disintegrating tablet of

pitavastatin calcium. *J Pharm Innov.* 2022 Sep;17(3):993–1010. <https://doi.org/10.1007/s12247-022-09661-x>

70. Arendrup MC, Cuenca-Estrella M, Lass-Flörl C, Hope W. EUCAST technical note on the EUCAST definitive document EDef 7.2: method for the determination of broth dilution minimum inhibitory concentrations of antifungal agents for yeasts EDef 7.2 (EUCAST-AFST). *Clin Microbiol Infect.* 2012 Jul;18(7):E246–7. <https://doi.org/10.1111/j.1469-0691.2012.03880.x>.
71. Grassiri B, Zambito Y, Bernkop-Schnürch A. Strategies to prolong the residence time of drug delivery systems on ocular surface. *Adv Colloid Interface Sci.* 2021 Feb;288:102342. <https://doi.org/10.1016/j.cis.2020.102342>.

Publisher's note

Springer Nature remains neutral with regard to jurisdictional claims in published maps and institutional affiliations.